ACS APPLIED POLYMER MATERIALS

pubs.acs.org/acsapm

Article

Comparative Study on Bioactive Filler/Biopolymer Scaffolds for Potential Application in Supporting Bone Tissue Regeneration

Micaela Degli Esposti,* Maryam Changizi, Roberta Salvatori, Luigi Chiarini, Valeria Cannillo, Davide Morselli,* and Paola Fabbri

Cite This: *ACS Appl. Polym. Mater.* 2022, 4, 4306−4318

Read Online

ACCESS | Metrics & More | Article Recommendations | Supporting Information

ABSTRACT: The combination of biopolymers and bioactive inorganic particles for bone tissue regeneration has been investigated in the last decades. However, several studies report discordant results on the specific synergistic effect of the compounds. A comparative study on porous scaffolds obtained by the combination of the most promising biopolymers and bioactive inorganic particles is herein reported. Specifically, porous scaffolds have been fabricated by the Thermally Induced Phase Separation method using poly(3-hydroxybutyrate-*co*-3-hydroxyvalerate) (PHBV), poly(lactic acid) (PLA), and poly(caprolactone) (PCL) compounded with hydroxyapatite (HAp), calcium silicate (CS), or a Mg- and Sr-rich bioglass (BG) with a nominal composition of 2.3% Na_2O, 2.3% K_2O, 25.6% CaO, 10.0% MgO, 10.0% SrO, 2.6% P_2O_5, and 47.2% SiO_2. Morphological analyses revealed the formation of highly interconnected and aligned open pores. Both thermal investigations and compressive tests highlight the close similarity between PLA- and PHBV-based scaffolds in terms of the amorphous structure and stiffness when the fillers are added. On the other hand, the addition of amorphous BG in semicrystalline PCL shows a decrease of the crystallinity degree of the polymer and a consequent decrease of the compressive modulus. Preliminary *in vitro* investigations (direct and indirect contact tests) carried out on the composite systems revealed that all the prepared materials provide an appropriate environment for NIH 3T3 cell adhesion and proliferation, showing a total lack of cytotoxicity. The addition of all the inorganic fillers has an overall positive effect on cell proliferation, viability (Neutral Red uptake), and metabolic activity (MTT test). Interestingly, this effect is particularly evident whenever BG is added. The combination of both amorphous BGs with amorphous polymers, such as PLA and PHBV, seems to be responsible for creating the best microenvironmental cue for NIH 3T3 cell attachment and proliferation.

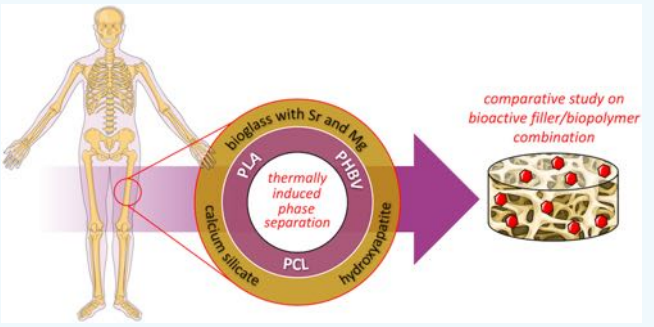

KEYWORDS: *scaffold, biopolymer, porous material, bicomposite, bioactive glass, bone regeneration*

1. INTRODUCTION

The prolonged life expectancy has led to a rapid increase of musculoskeletal pathologies in the last decades. Specifically, congenital defects, fractures, bone infections or cancers, oral and maxillofacial pathologies, and rheumatic diseases are among the most common cases where a suitable scaffold for bone tissue regeneration can play a very important role.[1] Several materials have been recently developed as active bioresorbable supports, which can be replaced by the growing cells. In an effort to improve cell adhesion and proliferation and avoid the negative outcomes derived from the non-acceptance or failure of the implant, a supporting material with a suitable porous structure and mechanical and chemical−physical properties is highly desirable.[2] In the design of a scaffold, a porous architecture that mimics the complex and hierarchical structure of the damaged or lost tissue is a key point. Open and fully interconnected pores are recognized to be pivotal to promote cell migration and ingrowth, nutrient transport, and metabolic waste removal through the material.[3] Another crucial aspect that has to be considered is the chemistry of the surface where the cells are seeded and grow, which makes the device actually effective.

A scaffold is typically composed of a biocompatible polymeric matrix with the addition of one or more active fillers, which are capable of promoting different properties such as improving mechanical strength, cell growth and adhesion, osteoinductivity, and osteoconductivity.[4−6]

Polymer-based composite scaffolds can satisfy most of the requirements of the application field. Most commonly, poly(lactic acid) (PLA), poly(caprolactone) (PCL), and poly(3-hydroxybutyrate-*co*-3-hydroxyvalerate) (PHBV)[3,7] are

Received: February 13, 2022
Accepted: May 9, 2022
Published: May 23, 2022

the studied biopolymers for this type of biomedical applications, thanks to their biocompatibility and bioresorbability. The incorporation of specific inorganic particles is a valuable approach to add new properties to the neat polymeric matrix. Among inorganic fillers, hydroxyapatite (HAp), calcium silicates (CSs), and bioglasses (BGs) are often used not only to tune the polymer thermo-mechanical properties[8,9] but also to promote osteogenesis, osteoconductivity, osteoinductivity, direct bonding to bone, and vascularization.[10−17]

Although a lot of studies have been reported in the recent years, there are still several unclear and often discordant results on the effect of the filler/polymer combination on the aforementioned properties since each work focuses on a specific composite combination, fabrication method, or testing condition.

In consideration of such inconsistencies, the herein proposed study aims at comparing, in terms of morphology, thermo-mechanical properties, and direct/indirect cytotoxicity of NIH 3T3 (mouse embryonic fibroblast) cells, biopolymer-based scaffolds filled with the three bioactive inorganic fillers. Specifically, highly porous scaffolds based on PHBV, PLA, and PCL and containing hydroxyapatite, calcium silicate, or a Sr- and Mg-rich bioactive glass were produced using the Thermally Induced Phase Separation (TIPS) technique and used under the same conditions to have no alteration of the scaffold due to the procedure and thus directly comparable results.

2. EXPERIMENTAL SECTION

2.1. Materials. A recently developed Sr- and Mg-rich bioactive glass was obtained from raw powder reagents. Such composition is referred to as BG from here on. The preparation is described in Section 2.2.

Hydroxyapatite (HAp, synthetic nanopowder, ≥97%, <200 nm particle size by BET), calcium nitrate tetrahydrate, and sodium metasilicate nonahydrate used for the synthesis of calcium silicate (CS) were purchased from Merck group, Italy.

Poly(3-hydroxybutyrate-*co*-3-hydroxyvalerate) (PHBV, custom grade, M_n 209,300, M_w 586,000, 20 mol % 3HV) and poly(caprolactone) (PCL, M_n 46,800, M_w 77,600) were purchased from Merck group, Italy. Poly(D,L-lactic acid) (PLA, Ingeo biopolymer PLA 4060D, M_n 103,100, M_w 232,900, copolymer ratio of D to L 12:88 mol %[18]) was kindly provided by Natureworks, USA. Before the scaffold fabrication, impurities or additives eventually present in the starting polymers and that can affect the studied properties were removed as described elsewhere.[19] In brief, as-received polymers were solubilized in warm $CHCl_3$, filtered through Celite, and precipitated in icy methanol. Molecular weights of the polymers were determined by gel permeation chromatography (GPC) as described in the Supporting Information and summarized in Table S1. Figure S1 reports purified PHBV, PLA, and PCL chromatograms. The molar content of 3-hydroxyvaleric acid (3HV) units of PHBV was assessed by proton nuclear magnetic resonance (^{1}H-NMR) as described in the Supporting Information. Figure S2 reports the ^{1}H-NMR spectrum of purified PHBV.

Chloroform ($CHCl_3$, HPLC grade), deuterated chloroform ($CDCl_3$, 99.8 atom% D, 0.03% vol/vol of TMS), 1,4-dioxane (DIOX, ≥99.0%), methyl alcohol (MeOH, ≥99.8%), ethyl alcohol (EtOH, 99.8%), and Celite (Standard Super Cel fine) were purchased from Merck group, Italy.

2.2. Bioactive Glass Preparation. The bioactive glass was produced by means of a classical melt quenching route, as illustrated in detail elsewhere[20] and here briefly summarized. The raw materials (namely, silicon dioxide, tricalcium phosphate, sodium carbonate, calcium carbonate, potassium carbonate, strontium carbonate, and magnesium hydroxide pentahydrate, all from Carlo Erba, Italy) were weighted, mixed for 2 h in a laboratory shaker, and then melted in air in a platinum crucible at 1450 °C in a furnace. The molten glass was then rapidly quenched in water to obtain a frit that was then dried at 110 °C for 14 h. Powders with a grain size below 63 μm were obtained after grinding (20 min, dry conditions) and sieving of the frit. The final composition of the BG was 2.3% Na_2O, 2.3% K_2O, 25.6% CaO, 10.0% MgO, 10.0% SrO, 2.6% P_2O_5, and 47.2% SiO_2.

2.3. Calcium Silicate Synthesis. The CS was synthesized by adjusting the procedure previously reported elsewhere.[21] In brief, to a 0.2 M calcium nitrate tetrahydrate solution (20 mL), a 0.01 M sodium hydroxide solution was added under stirring until pH 11.5 was reached. Then, a 0.2 M sodium metasilicate nonahydrate solution (20 mL) was added, and the suspension was stirred for 1 h by mechanical mixing to give a homogeneous system. The mixture was heated to 200 °C in an autoclave and then cooled to room temperature. After filtration, the solid residue was washed several times with Milli-Q water and recovered by centrifugation. The so obtained powder was dried at 100 °C for 24 h.

2.4. Scaffold Fabrication. The polymer-based composite scaffolds with 10 wt % of inorganic content were prepared by dispersing the selected inorganic particles in a purified polymer/DIOX solution (0.036 g·mL^{-1}). In particular, a given amount of inorganic filler was dispersed by magnetic stirring combined with dip-sonication using an ultrasonic processor (UP50H, Hielsher, sonotrode MS2) operating at 50 W and 30 kHz for 3 h (formulation details in Table 1). When PHBV was used, the dispersion took place under reflux. For comparison reasons, the same mixing conditions were used also for the production of neat polymer scaffolds (details in Table 1).

Table 1. Formulations Used for Scaffold Preparation

sample code	O:I ratio (wt %:wt %)	DIOX (mL)	polymer (g)	inorganic particles (g)
PHBV	100:0	25	0.9	-
PHBV-HAp	90:10	25	0.9	0.1
PHBV-CS		25	0.9	0.1
PHBV-BG		25	0.9	0.1
PLA	100:0	25	0.9	-
PLA-HAp	90:10	25	0.9	0.1
PLA-CS		25	0.9	0.1
PLA-BG		25	0.9	0.1
PCL	100:0	25	0.9	-
PCL-HAp	90:10	25	0.9	0.1
PCL-CS		25	0.9	0.1
PCL-BG		25	0.9	0.1

The Thermally Induced Phase Separation (TIPS) technique was used for obtaining the desired porous structure. In detail, after mixing, all the mixtures were placed into disposable aluminum molds and quickly cooled at −18 °C. After 18 h, the frozen samples extracted from the molds were soaked in icy EtOH for 72 h. To remove DIOX completely, EtOH was refreshed daily. Lastly, the solid scaffolds were carefully washed with cold Milli-Q water in an ultrasound bath and dried in an oven. Ten circular samples (diameter approx. 55 mm and thickness 10 mm) were prepared for each composition (Figure S3 of the Supporting Information reports representative photographs of the specimens).

The prepared scaffolds were coded as a "polymeric matrix-inorganic particle" that composes the sample.

2.5. Characterization. The morphology and dimensions of the inorganic particles were evaluated by transmission electron microscopy (TEM). In particular, a JEOL JEM-2010 TEM operating at 120 kV and a Thermo Fisher Scientific Talos F200S G2 operating at 200 kV were used for the analysis of commercial HAp, and synthesized CS and BG, respectively. Energy-dispersive X-ray spectroscopy (X-EDS, Thermo Fisher Scientific EDS system 2 SDD windowless design) was used in STEM mode for determining the atomic composition of CS and BG. 5 μL of a powder dispersion (approx. 0.002 g of powder in 2

https://doi.org/10.1021/acsapm.2c00270
ACS Appl. Polym. Mater. 2022, 4, 4306−4318

mL of EtOH, ultrasound mixing for 1 h) was dropped on a copper grid (300 mesh Cu carbon only) and dried at room temperature. The FIJI/ImageJ open-source software[22] was used for analyzing TEM images (approx. 30 particles were measured).

Inorganic fillers were investigated by means of X-ray diffraction (XRD) by a Philips PW3710 (Almelo, The Netherlands) X-ray diffractometer. Data collection was performed using a Cu Kα X-ray line by a 2θ scan method in the range of 5−70°.

An environmental scanning electron microscope (ESEM, Quanta-200 Fei , Oxford Instruments) connected to a backscattered electron detector was used for investigating the scaffold cross-section morphology without the application of a conductive coating. Samples were analyzed at low vacuum (75 Torr) applying 20 keV. When composite scaffolds were observed, energy-dispersive X-ray spectroscopy (X-EDS, INCA 350, Oxford Instruments) was used for determining the atomic composition. The FIJI/ImageJ open-source software was used for analyzing ESEM images. The average pore size as the mean from measures taken in three different areas of the samples (magnification from 200 to 500×) was estimated.

The open porosity (P_0) of the scaffolds was measured as specified by the standard procedure UNI EN 1936:2007.[23] Briefly, evacuated vessels (20 mbar) containing dry and weighted test samples (m_d, dry mass) were kept at the pressure of 20 mbar for 5 h for completely removing the air contained in the porosities. Milli-Q water was slowly introduced into the vessel, and the pressure was maintained at 20 mbar. When the water entirely covered the test specimens (approx. 30 min), the vessel was returned to the atmospheric pressure and the samples were left under water for 24 h. Then, the hydrostatic mass (m_h) was recorded by weighting the specimens under water. Finally, after a quick but gentle wipe with a dampened tissue paper, the saturated mass (m_s) was determined. The open porosity of the scaffolds was expressed as a percentage by the following equation:

$$P_0 = (m_s - m_d)/(m_s - m_h) \times 100 \quad (1)$$

Mean values were calculated from three measurements and expressed as mean ± standard deviation.

A dynamic mechanical instrument (Q800, DMA, TA Instruments) equipped with a compression clamp (40 mm disc diameter) was used for investigating the mechanical properties of the scaffolds. Analyses were performed on square-shaped samples (approx. width 20 mm and thickness 10 mm) at 35 °C and in controlled force mode. A preload of 0.005 N and a force ramp rate of 1 N·min^{-1} were applied. The compressive modulus was calculated as the slope of the linear elastic region of the stress−strain curve (between 0.05 and 0.25% of strain). The TA Universal Analysis 2000 Version 4.5A software (TA Instruments) was used for data analysis.

A differential scanning calorimeter (DSC, Q10) equipped with a Discovery Refrigerated Cooling System RCS90 (all TA Instruments) was used for investigating the thermal properties of the produced scaffolds. The instrument was calibrated in temperature and enthalpy with an indium standard, and nitrogen was used as purge gas (50 mL·min^{-1}). Samples of about 9 mg were placed in an aluminum pan and cooled down rapidly to −90 °C at 30 °C·min^{-1}. Then, one heating cycle from −90 to 195 °C (hold for 2 min) followed by a cooling scan from 150 to −90 °C and a second heating scan from −90 to 150 °C was applied with heating and cooling rates of 10 °C·min^{-1}. DCS curves were analyzed by the TA Universal Analysis 2000 software to extrapolate the melting temperatures (T_m), cold crystallization temperatures (T_{cc}), and enthalpies of melting (ΔH_m) from heating scans. Crystallization temperatures (T_c) were extrapolated from cooling scans. Glass transition temperatures (T_g) were extrapolated during both heating and cooling scans. The percentage of crystallinity was calculated for PHBV- and PCL-based materials by the following equation:

$$\chi_c = [(\Delta H_m)/(\Delta H^0{}_m W)] \times 100 \quad (2)$$

where χ_c is the percentage of crystallinity, ΔH_m is the experimental enthalpy of melting recorded during heating scans, and $\Delta H^0{}_m$ is the melting enthalpy for the 100% crystalline polymer ($\Delta H^0{}_m$ = 109 and 136 J·g^{-1} were used for PHBV and PCL, respectively).[24,25] W is the weight fraction of the polymer in the composites (W = 1 for neat polymers).

2.6. Biological Tests. The scaffolds' biocompatibility was evaluated *in vitro* utilizing NIH 3T3 cells, which are mouse embryonic fibroblast cells. The cytotoxicity was investigated according to the standard procedure ISO 10993, in particular, (a) 10993-1[26] for the selection of tests, (b) 10993-12[27] for sample preparation and reference materials, and (c) 10993-5[28] for the *in vitro* methods.

Both the direct and indirect contact tests were employed to assess the cytotoxicity and biocompatibility of the scaffolds. In particular, the Neutral Red (NR) uptake assay and MTT assay were used. The Neutral Red uptake assay enables to distinguish between viable cells and damaged or dead cells by investigating the incorporation of neutral red dye into cells by means of optical density measured by spectrophotometry. On the other hand, the MTT assay quantifies formazan accumulated into metabolically lively cells using a spectrophotometer.

NIH 3T3 mouse fibroblasts (Zooprophylactic Experimental Institute of Brescia, Italy) were grown in the minimal essential medium of Dulbecco (DMEM) containing 10% vol/vol of fetal bovine serum, 100 U·mL^{-1} penicillin, and 100 U·mL^{-1} streptomycin at 37 °C in a 5% CO_2 atmosphere. Once confluence was reached, cells were trypsinized, washed in Dulbecco's phosphate buffer solution (D-PBS), resuspended in DMEM, and seeded at 1 × 10^5 cells·mL^{-1} in 12-well multiwell dishes. The samples were first sterilized by UV rays for 1 h under a laminar flow cabinet, and then they were placed in 12-well plates. Cells were cultured in an incubator (at humidity of 90 ± 5%, temperature of 37 ± 1 °C, and CO_2/air ratio of 5 ± 1%). After 24, 48, and 72 h, cells were observed under an optical microscope (Leitz, Germany) to check the morphology (eventual presence of damage to the cell membrane, cytoplasm, swelling, or debris). As a negative control (CTRL−), DMEM only was used. Latex samples (Sensichlor powder free, lot 45126) were used with the ratio 3 cm^2·mL^{-1} (surface of sample/liquid volume) as a positive control (CTRL +). The same CTRL− and CTRL+ were also used in the subsequent tests.

Scaffolds were cut by using a razor blade in smaller blocks, having a squared base of approximately 16 × 16 mm^2 and a 10 mm height. Cells were cultured in direct contact with scaffolds in 12-well plates, as described previously. After 24, 48, and 72 h of cell culture, the NR uptake assay was carried out to evaluate cell viability according to the ISO protocol.[26,28] Briefly, 150 μL of the NR solution (3.3 g·L^{-1} in D-PBS, Merck group, Germany) was added to each well and incubated at 37 °C for 3 h. After each incubation time (i.e., 24, 48, and 72 h), wells were washed twice with D-PBS to remove the excess of the NR solution. Then 1.5 mL of the extracting mixture (EtOH/glacial acetic acid) was added to each well in a ratio of 1:1 to extract the NR dye from cells. Afterward, 100 μL of the supernatant of each well was transferred to a 96-well plate, and the amount of NR dye bound by cells was measured at 540 nm using a microplate spectrophotometer (Thermolab system, Finland).

To test the indirect cell viability, an MTT assay was performed using NIH 3T3 as well. The preparation of eluates was carried out according to the ISO protocol.[27] Squared base scaffolds as detailed above were immersed in a volume of DMEM with a 3 cm^2·mL^{-1} ratio between the standard surface and liquid volumes. Samples were incubated for 72 h at 37 °C. Then, before MTT testing, scaffolds' eluates were filtered with a Millipore filter (Millex Gs 0, 22 μm, Millipore, France). Cells were seeded in a 96-well multiwell dish at a concentration of 5000 cells·mL^{-1}. Fifty microliters of eluates of the prepared samples was added to each well. After 24, 48, and 72 h of incubation, 10 μL of tetrazolium salts (5 mg·5 mL^{-1} in PBS) was poured into each well and incubated for 2 h at 37 °C. At the end of the incubation, the supernatant was removed and 100 μL of DMSO was added to each well to dissolve the formazan crystals. Finally, to quantitatively determine the concentration of formazan synthesized inside cells, the absorbance was measured at 540 nm (for each well).

All experiments were performed in triplicate. Data were expressed as mean ± standard deviation. The Student t test was performed to

https://doi.org/10.1021/acsapm.2c00270
ACS Appl. Polym. Mater. 2022, 4, 4306−4318

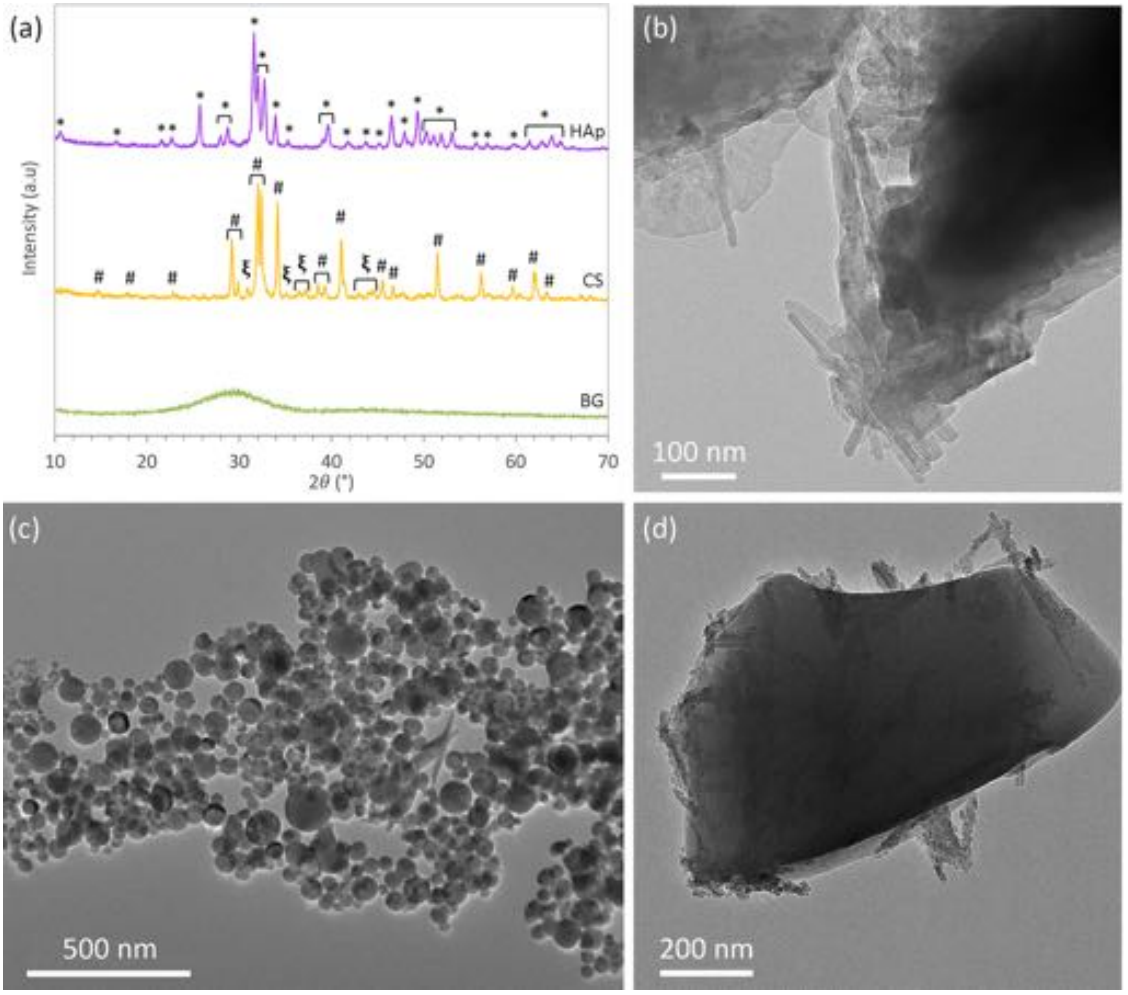

Figure 1. (a) XRD diffractograms of the bioactive fillers HAp, CS, and BG. HAp reference pattern ICDD: 96-900-3550 (*), dicalcium silicate reference pattern: 01-083-0461 (ξ), and tricalcium silicate reference pattern: 01-070-1846 (#). Representative TEM micrographs of (b) CS, (c) HAp, and (d) BG at different magnifications.

compare data between composite scaffolds and the corresponding neat polymer. $p < 0.05$ was considered statistically significant.

3. RESULTS AND DISCUSSION

3.1. Material Preparation and Characterizations. In this study, experimental PHBV-, PLA-, and PCL-based composite scaffolds were prepared by the addition of 10 wt % of bioactive commercial hydroxyapatite, synthesized calcium silicate, or a Mg- and Sr-rich bioactive glass. The typical fraction of inclusions is 0−30 wt %,[29,30] but it is reported by many authors[19,31] that smaller filler amounts (i.e., 10 wt %) offer a good balance between improved thermo-mechanical properties and a favorable environment for cell growth, adhesion, and differentiation, also preventing particle agglomeration and their inhomogeneous distribution in the polymer matrix.

Concerning the tested inorganic fillers, the broadened reflections of the XRD diffractograms presented in Figure 1a suggest that both HAp and CS are nanocrystalline materials. On the other hand, BG only shows two broad bands typical of amorphous glass-like materials. Furthermore, it was found that the diffractogram of HAp matches the hexagonal crystalline structure pattern of the reference hydroxyapatite (ICDD: 96-900-3550). Synthesized CS powder is mainly composed of tricalcium silicate (reference 01-070-1846) as clearly shown by the diffractogram in Figure 1a. Only low-intensity signals can be observed for the main peaks associated with dicalcium silicate (reference 01-083-0461), suggesting that this component is a minor portion.

Figure 1b−d depicts the morphology and dimensions of the inorganic particles resulting from TEM investigations. In detail, Figure 1b reveals that CS particles are organized in aggregates and that the primary particles present a rod-like morphology (length of 75−100 nm and diameter of 9−20 nm). HAp particles reported in Figure 1c show a spherical shape (< 100 nm in diameter with few bigger particles of 100−150 nm), but few needles are also observed. BG particles show an irregular shape (Figure 1d) and a grain size of approx. 1 μm × 600 nm. Moreover, X-EDS spectra (Figure S4) performed on the synthesized CS and BG particles shown in Figure 1b,d further support the results of the XRD measurements showing the expected elemental composition.

Highly porous composite scaffolds were fabricated using the Thermally Induced Phase Separation (TIPS) technique under the same conditions to have no alteration of the scaffold due to the procedure and thus directly comparable results. Thanks to its simple experimental procedure and the fact that there is no need to use high temperatures that may modify the properties of both the polymeric matrix and filler, TIPS represents an interesting strategy to fabricate highly porous structures.[32−34]

https://doi.org/10.1021/acsapm.2c00270
ACS Appl. Polym. Mater. 2022, 4, 4306−4318

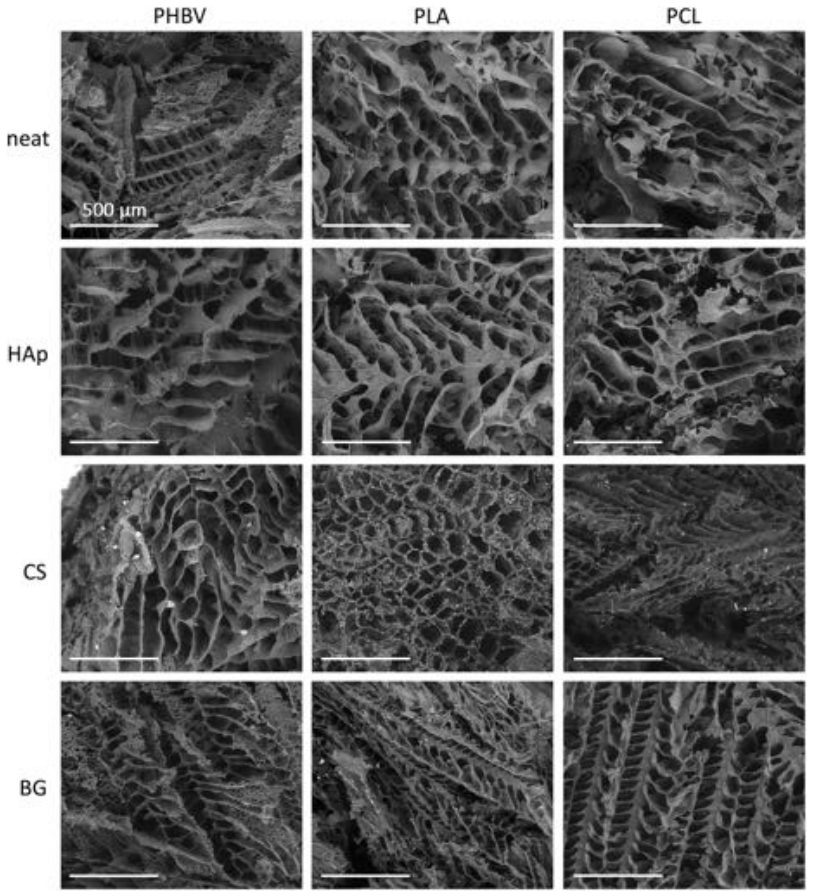

Figure 2. Cross-section ESEM micrographs recorded by a backscattered electron detector of all the prepared compositions at 200× magnification (all markers correspond to 500 μm).

Moreover, the combination of mechanical and ultrasound mixing for the dispersion of the inorganic filler allows the preparation of homogeneous samples with good filler distribution and limited particle aggregation.

Pore architecture, pore size, and pore distribution, as well as the total open porosity, are among the most important parameters that play a critical role in balancing the physical−mechanical and biological properties of the scaffold. Even if it is difficult to define the ideal porosity features for a model scaffold, high and open porosity is required to allow the proper tissue ingrowth, vascularization of the implant, flow of nutrients, and removal of wastes derived from metabolic activity through the scaffold.[35−37] Generally, large pores (hundreds of microns, macroporosity) seem to be mainly associated with high cell seeding efficiency and penetration. On the other hand, a smaller porosity (from nanometers up to several microns, microporosity) seems to affect mainly the ability of cells to proliferate and differentiate. Highly porous materials, thanks to a larger surface area, offer greater attachment opportunities for the adsorption of proteins involved in apatite formation and bone induction processes. Moreover, the proliferation and differentiation of cells are favored by a rough surface.[38]

For this reason, the morphology of the produced scaffolds was investigated by ESEM analysis. As observed in Figure 2, ESEM micrographs (200×) performed on the scaffolds' cross-sections reveal high and interconnected porosity for all the prepared compositions. Independently of the polymer matrix and the added filler, the scaffolds are characterized by pores of hundreds of micrometers. More in detail, smaller porosities are also detectable in PHBV-based scaffolds, which are characterized by microporosity of few microns in size.

With the exception of the composition PLA-CS that shows an almost circular porosity, directionally oriented oblong pores typically formed by solid−liquid phase separation guided by solvent crystallization are observed.[39] Indeed, Jack and co-workers[40] have already reported a similar microtubular architecture of parallel arrays for PHA copolymers containing HV blocks, whereas Ma's research unit[41−43] has observed the same arrangement for PLA-based scaffolds prepared by TIPS when a rapid cooling rate is used during the scaffold fabrication. Specifically, all PHBV scaffolds present oblong pores aligned in columns in the range of hundreds of microns (average pore dimensions of approx. 100 × 70 μm), but microporosity (≤10 μm) is also observed especially in the neat PHBV and in BG- and CS-containing scaffolds. Oblong pores arranged in columns are also detected in PLA- and PCL-based compositions. Macropores (range 150 × 70 μm) and micropores (range 70 × 30 μm) in PLA-based scaffolds are arranged in short (neat PLA and PLA-HAp) and longer columns (PLA-BG). PLA-CS shows a completely different arrangement, and almost circular and non-aligned pores can be detected with dimensions ranging from 70 to 30 μm, but few larger pores (approx. 150 × 90 μm) are also observed. Concerning PCL-based scaffolds, the neat PCL and HAp- and CS-containing scaffolds show few larger pores (approx. 200 × 100 μm) even though the porosity dimension is mainly in the range from 90 to 30 μm. For PCL-BG, a regular ladder-like

https://doi.org/10.1021/acsapm.2c00270
ACS Appl. Polym. Mater. 2022, 4, 4306−4318

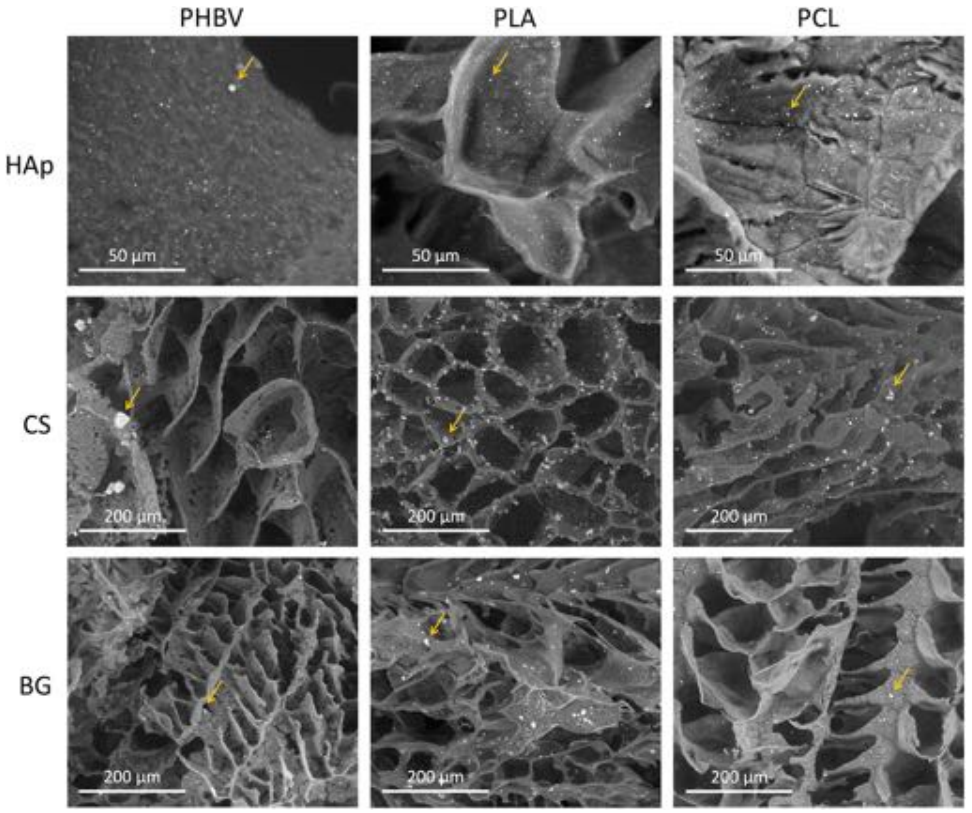

Figure 3. Cross-section ESEM micrographs (backscattered electrons) at 2000× magnification for HAp and 500× magnifications for CS and BG. Orange arrows identify the points of punctual X-EDS analysis (shown in Figure S5).

pore architecture is detected with average pore dimensions of 100 × 40 μm. Microporosity is not observed in all PLA- and PCL-based scaffolds. On the basis of the ESEM investigations, the introduction of the filler and the filler type seem not to modify the pore architecture and pore size observed for the neat compositions.

The remarkably high level of open porosity measured for all the prepared scaffolds by eq 1 (92−95%, Table S2) further confirms that the TIPS technique is an effective and reliable strategy for the production of porous materials with an extremely high level of open pores.

Filler dispersion is still one of the main goals dealing with composite materials especially when the filler is not introduced in the polymer matrix by *in situ* synthesis. To prevent inorganic particle aggregation and improve their dispersion, mechanical mixing was coupled with ultrasound mixing during the TIPS preparation procedure. Cross-section ESEM micrographs of the composite scaffolds (Figure 3) reveal that the strategy of coupling magnetic stirring with ultrasound mixing during TIPS preparation was effective to prevent inorganic particle aggregation and improve filler dispersion. Nevertheless, when CS was used as a filler in PHBV, some big aggregates (18−25 μm) were observed. Punctual X-EDS spectra (Figure S5) show the expected elemental composition.

Besides the high and interconnected porosity required for tissue proliferation and differentiation shown by the prepared scaffolds, the high porosity may lead to a detrimental effect on the mechanical properties. With the aim of evaluating the mechanical behavior of the prepared materials, compression tests were carried out. As reported in Figure 4 and summarized in Table S2, comparable compressive results are observed for PHBV- and PLA-based materials (Figure 4a,c). In comparison to the neat composition, the expected reinforcing action of the inorganic fillers HAp and BG on the polymeric matrices is confirmed by the increased values of compressive moduli (Figure 4b,d). On the contrary, the addition of CS does not improve the stiffness. In particular, the presence of some filler aggregates in the PHBV-CS sample (shown in Figure 3) may have compromised the expected reinforcing effect. A different compressive behavior is observed for PCL-based materials (Figure 4e). Surprisingly, the addition of no one of the inorganic fillers to PCL has led to an increase of the compressive modulus (Figure 4f). Indeed, when comparing the neat PCL to the BG-doped composition, the compressive modulus is almost halved when the filler is added. The inclusion of HAp and CS leads to comparable modulus values and to a slight decrease of stiffness with respect to the neat PCL. The higher stiffness of the neat PCL can be explained by considering the value of open porosity (Table S2), which is lower with respect to the doped compositions.

All the measured compressive moduli are less than 5 MPa and are compatible with previously published results for similar systems.[44−46] In spite of the very much lower compressive moduli typically observed for cortical and cancellous bone (12−20 GPa and 100−500 MPa, respectively[3,47−49]), the prepared scaffolds are not proposed for load-bearing applications but intended for soft-tissue engineering and maxillofacial application, for orbital implants, and as bone fillers as proposed by other authors.[44] Moreover, the prepared materials can be handled freely during characterization and biological tests without the risk of collapse.

The materials' thermal history is a very important issue that influences the arrangement of amorphous/crystalline phases and the physical−mechanical properties of the material. As can

https://doi.org/10.1021/acsapm.2c00270
ACS Appl. Polym. Mater. 2022, 4, 4306−4318

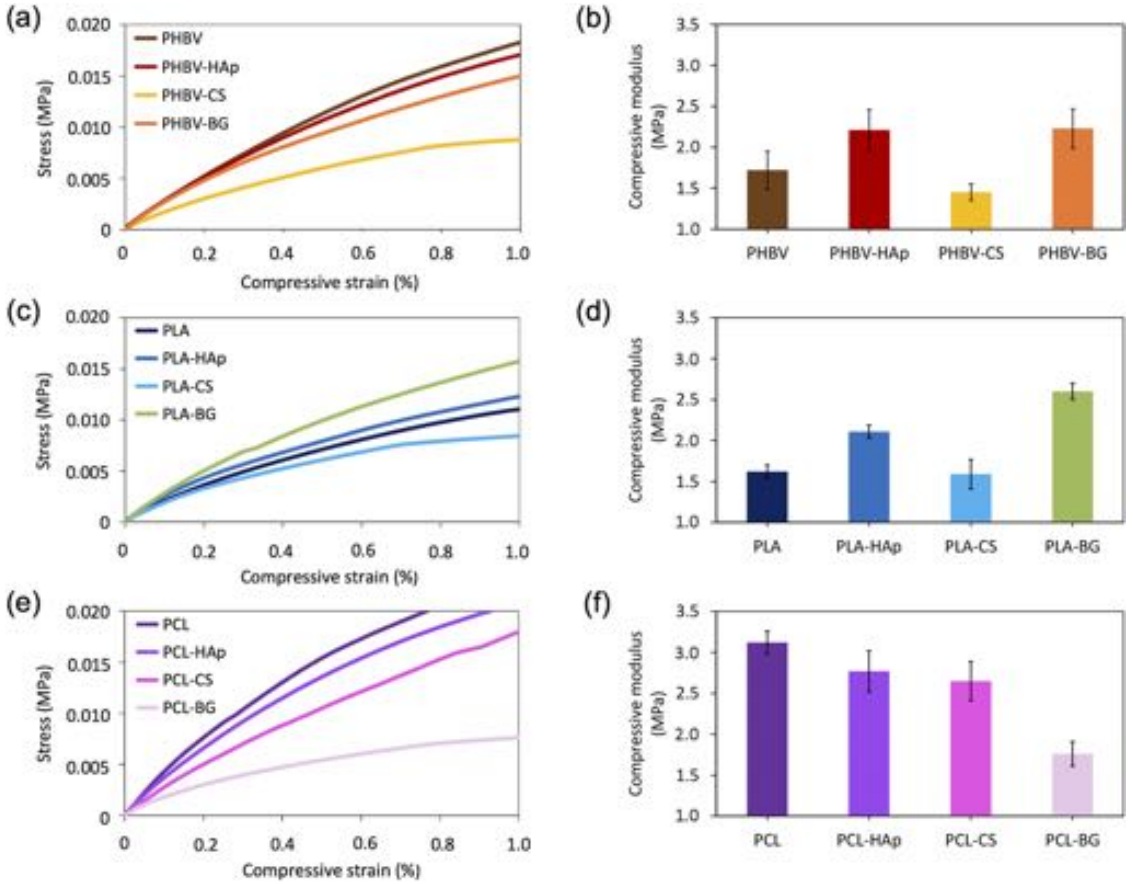

Figure 4. Average compression stress−strain curves and compressive moduli for (a, b) PHBV-, (c, d) PLA-, and (e, f) PCL-based materials, respectively.

be seen from Figure 5, which reports DSC curves, and Table S3, which summarizes the DSC results, PHBV-based materials feature the same thermal profile with no substantial differences. As expected, the introduction of hydroxyvaleric units (20 mol % 3HV) limits the polymer ability to crystallize[50] and leads to an almost amorphous structure. Indeed, during the first heating scan, a very small melting peak that corresponds to 1% of crystallinity is observed for the neat PHBV. The addition of inorganic fillers is not able to increase this value by acting as a nucleating agent, and it does not have any effect on the T_m (164−165 °C). Noise is detected between 30 and 120 °C. The crystallization occurs during the reheating stage as cold crystallization (80−85 °C). Glass transition temperatures are observed during all the analyzed scans. Independently from the filler addition and the filler type, similar T_g values are observed (−1 to 1, −13 to −9, and − 9 to −5 °C for the first heating, first cooling, and second heating scans, respectively). PLA-based compositions show a completely amorphous behavior during all the analyzed scans. The filler addition and filler composition seem not to affect glass transition; similar T_g values are recorded during both cooling and heating scans (53−60, 51−52, and 56−58 °C for first heating, cooling, and second heating, respectively) for all the prepared compositions even if a small decrease in the T_g value is observed during the first heating when BG is added with respect to the neat PLA. The neat and doped PCL scaffolds are semicrystalline materials for which melting and crystallization peaks are observed during heating and cooling scans, respectively. Similar melting temperatures in the range 61−63 and 57−58 °C for the first and second heating scan, respectively, are observed for all PCL-based scaffolds. No significant variations are detected for T_c values (28−31 °C), but a decrease in crystallinity is observed for composites (62−57 and 42−36% calculated during the first and second heating, respectively) when compared to the neat PCL (65 and 43% calculated during the first and second heating, respectively). It is worth noting that the crystallinity degree is reduced by approx. 10% (Table S3) when amorphous BG has been added to the semicrystalline polymer as PCL. This finding can explain the reduction of the compressive modulus and the detrimental effect on the stiffness of PCL-BG with respect to the neat composition (Figure 4f and Table S2). On the other hand, the addition of amorphous BG to amorphous polymers as PHBV and PLA leads to an increase of the compressive moduli.

3.2. Biological Tests. NIH 3T3 cells cultured on the different samples were observed by means of optical microscopy. The morphology of NIH 3T3 cells seeded on the three different polymer-based systems is similar (no lysis or rounding appearance) to that on CTRL− at the three investigated time points (24, 48, and 72 h), as depicted in Figure 6. Thus, all the compositions were able to support NIH 3T3 adhesion and proliferation; this confirms the biocompatibility and absence of cytotoxicity of the scaffolds.

The results of the NR tests are illustrated in Figure 7, where all the values are normalized with respect to the negative control (CTRL−), which is set equal to 100. The Student t test was performed with reference to the unreinforced polymer. The NR test confirmed the results obtained by the observation

https://doi.org/10.1021/acsapm.2c00270
ACS Appl. Polym. Mater. 2022, 4, 4306−4318

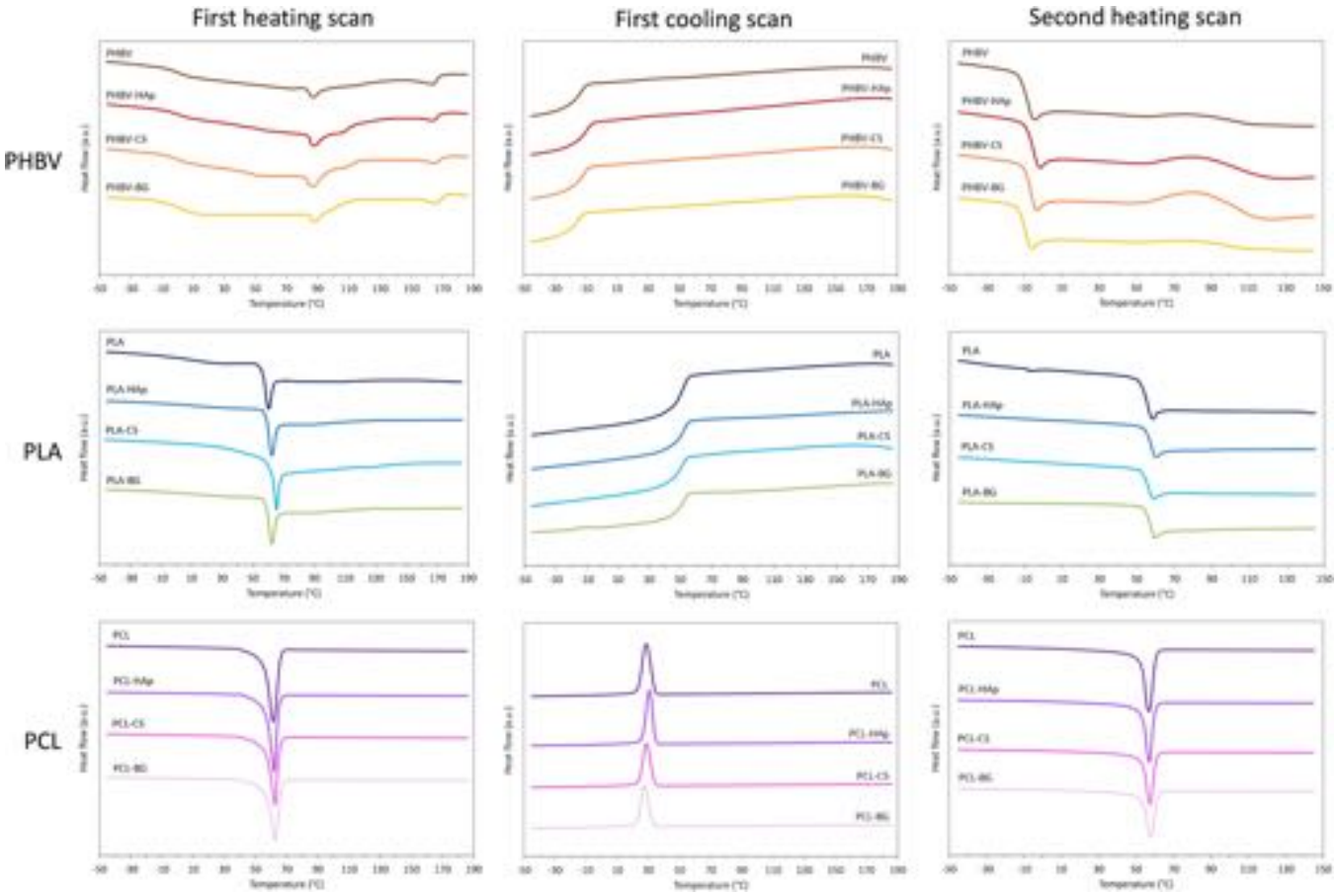

Figure 5. DSC curves recorded for PHBV-, PLA-, and PCL-based scaffolds during the first heating, first cooling, and second heating scans. Endothermic transitions are displayed by negative peaks in DSC curves.

of the morphology of cells. In fact, no significant decrease in lysosomal activity imputable to cytotoxicity was observed, thus evidencing the good biocompatibility. For both PHBV- and PLA-based doped scaffolds (Figure 7a,b), it can be noticed that the cellular viability increases with time, and this suggests the positive effect of the inorganic phase, especially BG, on the scaffold's biocompatibility. Therapeutic ions such as Mg and Sr contained in BG are prone to enhance cellular viability and tissue regeneration, as already reported in literature.[51] The dissolution of ions from the bioactive glass stimulates osteogenesis and angiogenesis both *in vitro* and *in vivo*. In particular, the synergistic effect of Ca, P, Si, Sr, and Mg ions improves cell proliferation and differentiation and, at the same time, is able to stimulate the genes' expression related to osteoblastic differentiation and antibacterial action.[52] As a matter of fact, Ca ions play an important role in cells and living systems, especially for bone tissue,[53] since Ca is one of its most important components. P ions, besides being involved in physiological processes, regulate the differentiation and mineralization of osteoblasts.[54] On the other hand, Si influences the metabolic process of bone forming, increases bone density, and induces collagen I production.[55,56] Sr stimulates cell proliferation, osteogenesis, and angiogenesis, enhancing osteoblast differentiation and stimulating bone formation,[52] and is already used in the treatment of osteoporosis (in the form of strontium ranelate). Moreover, the contemporary release of Sr and Si ions results in a synergistic effect on osteogenesis and angiogenesis.[52] Mg is able to stimulate proliferation and differentiation of stem cells and, by enhancing ALP activity, can play a pivotal role in bone metabolism.[57] Furthermore, it is well known that Sr and Mg ions promote specific cellular responses.[51] Indeed, BG resulted in a very promising composition, suitable for the preparation of powders, granules, coatings, dental putties, wound dressings, composite systems, and scaffolds, giving also a very positive response in innovative three-dimensional *in vitro* models with human mesenchymal stem cells.[20,58−64]

As pointed out by many authors, the mechanisms that regulate the scaffold's bioactivity and cell-mediated functions are related not only to the chemical composition but also to the microstructure, surface's features, and thermo-mechanical properties.[65−67] Specifically, Cui and Sinko[68] have observed that highly crystalline poly(caprolactone-*co*-glycolide) surfaces were significantly more efficient in supporting fibroblast growth thanks to their mechanical properties. Washburn *et al.*[69] have observed that MC3T3-E1 osteoblastic cells are much more sensitive to what they call the topography of the surface such as the roughness.

Interestingly, we have also noticed that the combination of the amorphous inorganic filler BG as observed by XRD analysis with the amorphous polymer matrices PLA and PHBV seems to offer the best biological outcome among the tested blends. Indeed, as experimentally observed by DSC, PLA and PHBV behave similarly in terms of the amorphous structure (PLA is completely amorphous, and PHBV is almost completely amorphous, showing only 1% of crystallinity).

https://doi.org/10.1021/acsapm.2c00270
ACS Appl. Polym. Mater. 2022, 4, 4306−4318

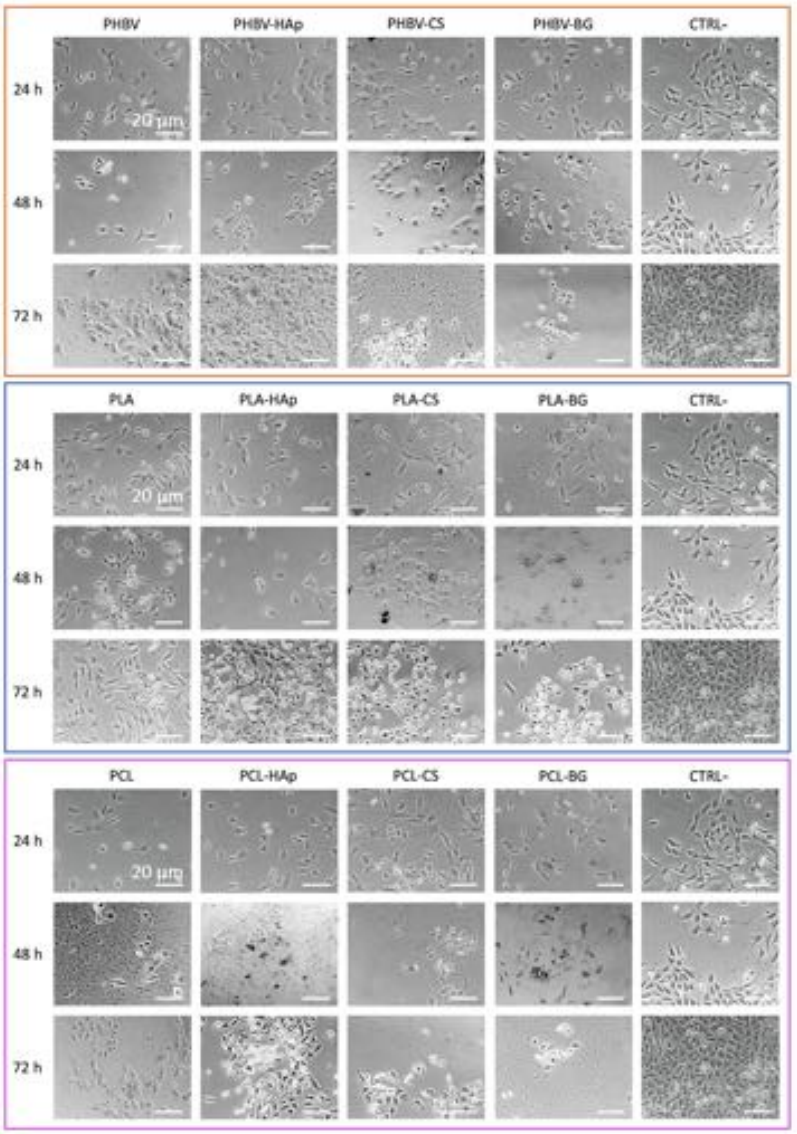

Figure 6. Morphological evaluation of cells in direct contact with the neat and composite scaffolds by optical microscopy at 24, 48, and 72 h after seeding. DMEM was used as negative control (CTRL−) (all markers indicate 20 μm).

Moreover, PLA-BG and PHBV-BG have similar mechanical properties as shown by compression tests. These results, together with the microstructural pattern offered by aligned pores as observed by ESEM investigations for these compositions, seem to be responsible for creating the best microenvironmental cue that favors the higher viability of NIH 3T3 among the tested compositions.

A different result is obtained with semicrystalline PCL (Figure 7c), where the beneficial effect of fillers is not completely clear. In fact, PCL-HAp, PCL-CS, and PCL-BG seem to have a better cellular viability than pure PCL at 24 h, especially for the composite with BG, but this is not confirmed for longer times. This feature needs to be deeply investigated, for example, by means of *in vivo* tests (in animals).

To further investigate the biocompatibility of the composite systems, an MTT assay was performed. It is important to point out that the MTT assay is also relevant to exclude any potential problem caused by particulate release from the scaffolds. As illustrated in Figure 8, which reports the outcomes of the MTT test, it is noteworthy to mention that none of the composite is cytotoxic. As for PHBV-based materials (Figure 8a), CS- and BG-containing scaffolds show at 24 h a better performance, which is confirmed also for longer times for the BG-doped composition: as a matter of fact, 72 h after contact with the PHBV-BG eluate, there is a positive cellular response compared to the neat PHBV. On the other hand, as already pointed out by Groussard and co-workers,[70] PLA degrading acts as an energy source for cells and protects them from free radicals. This probably explains why the addition of fillers did not substantially modify the good cell viability that the PLA eluate shows in culture (Figure 8b). With regard to the PCL composites (Figure 8c), 24 h after seeding, both PCL-HAp and PCL-BG exhibit a higher cellular viability in comparison to the neat PCL. However, for longer times, the cellular viability tends to decrease (as already observed in the direct NR test) even if all the samples show cytocompatibility for all the investigated times.

https://doi.org/10.1021/acsapm.2c00270
ACS Appl. Polym. Mater. 2022, 4, 4306−4318

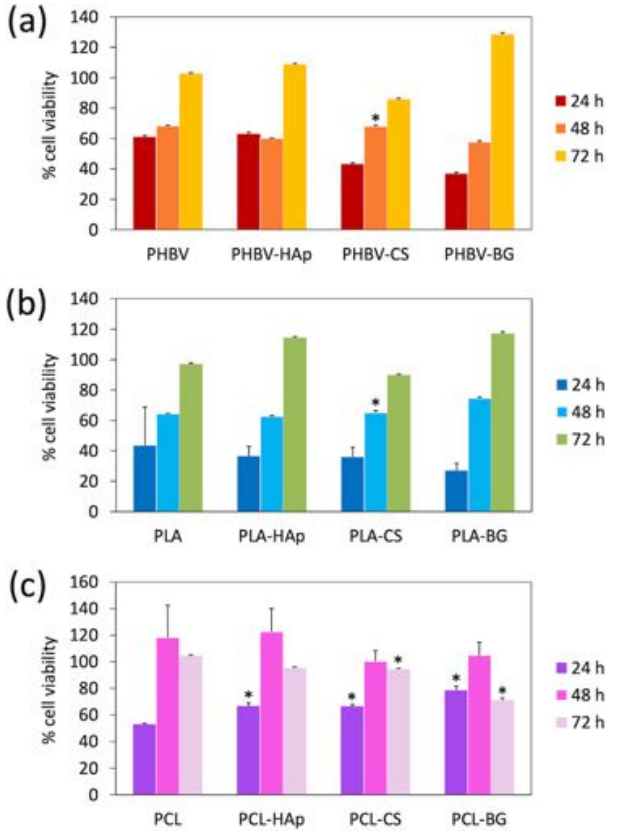

Figure 7. Neutral red (NR) uptake 24, 48, and 72 h after seeding for (a) PHBV-, (b) PLA-, and (c) PCL-based scaffolds. All the values are normalized with respect to the negative control (CTRL−) that is set equal to 100 (*p < 0.05).

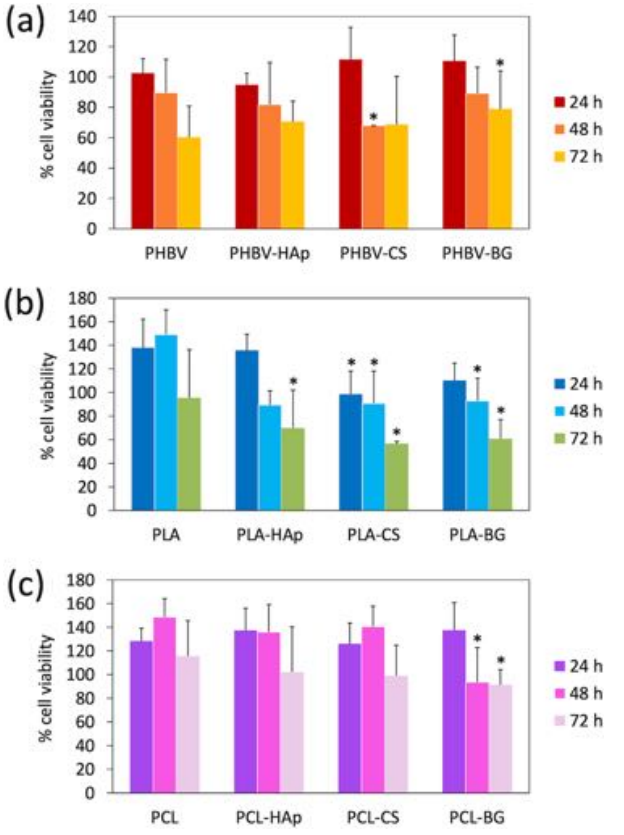

Figure 8. MTT test 24, 48, and 72 h after seeding for (a) PHBV-, (b) PLA-, and (c) PCL-based scaffolds. All the values are normalized with respect to the negative control (CTRL−) that is set equal to 100 (*p < 0.05).

4. CONCLUSIONS

3D highly porous composite scaffolds based on PHBV, PLA, and PCL and filled with 10 wt % of HAp, calcium silicate, or a Sr- and Mg-rich bioactive glass were fabricated using the Thermally Induced Phase Separation (TIPS) technique.

Morphological analyses revealed the formation of highly interconnected open porosity (close to 95%) with directionally oriented oblong pores, confirming the reliability of the TIPS technique to produce interconnected porous structures in the same experimental conditions. The addition of the fillers does not significantly affect the porosity and morphology of the porous structures.

Thermal investigations and compressive tests highlight the similar thermal and mechanical behavior of the amorphous PLA- and PHBV-based scaffolds. As expected, the addition of the fillers has a reinforcing effect, but when filler agglomeration is observed as for PHBV-CS, a detrimental effect on the stiffness is observed. On the contrary, PCL-based scaffolds are semicrystalline materials and none of the added fillers acts as a nucleating agent, thus decreasing the polymer crystallinity and compressive modulus.

Preliminary *in vitro* investigation (direct and indirect contact tests) carried out on the porous composites revealed that all prepared materials provide an appropriate environment for NIH 3T3 cell adhesion and proliferation, showing a total lack of cytotoxicity. The addition of all the inorganic fillers to PHBV, PLA, and PCL proved to be stimulating in cell proliferation in terms of both viability (NR uptake) and metabolic activity (MTT test). This effect is particularly evident whenever the amorphous bioactive glass BG is used in combination with amorphous polymers such as PLA and PHBV. In particular, PHBV-BG and PLA-BG show the highest viability (NR uptake). At 72 h, these compositions achieve the most successful balance between chemical composition, thermo-mechanical properties, and microstructural pattern offered by aligned pores, providing the best platform for cell attachment and proliferation.

■ ASSOCIATED CONTENT

Supporting Information

The Supporting Information is available free of charge at https://pubs.acs.org/doi/10.1021/acsapm.2c00270.

Gel permeation chromatography experimental procedure; molecular weights of the used polymers; chromatograms of the used polymers; proton nuclear magnetic experimental procedure; ^{1}H-NMR spectrum of PHBV; representative photograph of the prepared scaffolds; X-EDS analyses of the synthesized inorganic fillers; open porosity and compressive moduli of the prepared scaffolds; punctual X-EDS of the inorganic particles embedded into the scaffolds; and thermal properties of the prepared scaffolds (PDF)

■ AUTHOR INFORMATION

Corresponding Authors

Micaela Degli Esposti − *Department of Civil, Chemical, Environmental, and Materials Engineering, Università di*

https://doi.org/10.1021/acsapm.2c00270
ACS Appl. Polym. Mater. 2022, 4, 4306−4318

Bologna, 40131 Bologna, Italy; National Interuniversity Consortium of Materials Science and Technology (INSTM), 50121 Firenze, Italy; orcid.org/0000-0002-4513-8527; Email: micaela.degliesposti@unibo.it

Davide Morselli − *Department of Civil, Chemical, Environmental, and Materials Engineering, Università di Bologna, 40131 Bologna, Italy; National Interuniversity Consortium of Materials Science and Technology (INSTM), 50121 Firenze, Italy;* orcid.org/0000-0003-3231-7769; Email: davide.morselli6@unibo.it

Authors

Maryam Changizi − *Department of Civil, Chemical, Environmental, and Materials Engineering, Università di Bologna, 40131 Bologna, Italy;* Present Address: Department of Environmental and Infrastructure Engineering, Politecnico di Milano, Via Golgi 39, 20133 Milano, Italy

Roberta Salvatori − *Biomaterials Laboratory, Department of Medical and Surgical Sciences of Children and Adults, Università di Modena e Reggio Emilia, 41125 Modena, Italy*

Luigi Chiarini − *Biomaterials Laboratory, Department of Medical and Surgical Sciences of Children and Adults, Università di Modena e Reggio Emilia, 41125 Modena, Italy*

Valeria Cannillo − *National Interuniversity Consortium of Materials Science and Technology (INSTM), 50121 Firenze, Italy; Department of Engineering "Enzo Ferrari", Università di Modena e Reggio Emilia, 41125 Modena, Italy*

Paola Fabbri − *Department of Civil, Chemical, Environmental, and Materials Engineering, Università di Bologna, 40131 Bologna, Italy; National Interuniversity Consortium of Materials Science and Technology (INSTM), 50121 Firenze, Italy;* orcid.org/0000-0002-1903-8290

Complete contact information is available at: https://pubs.acs.org/10.1021/acsapm.2c00270

Author Contributions

Conceptualization: M.D.E. and D.M.; methodology: M.D.E. and D.M.; investigations: M.D.E., M.C., and R.S.; data curation: M.D.E. and D.M.; writing original draft: M.D.E., D.M., V.C., and R.S.; writing review: M.D.E., D.M., and V.C.; supervision: M.D.E., D.M., and V.C.; funding: P.F., V.C., and L.C.

Funding

This research did not receive any specific grant from funding agencies in the public, commercial, or not-for-profit sectors.

Notes

The authors declare no competing financial interest.

REFERENCES

(1) Agarwal, R.; García, A. J. Biomaterial Strategies for Engineering Implants for Enhanced Osseointegration and Bone Repair. *Adv. Drug Delivery Rev.* **2015**, *94*, 53−62.

(2) Chan, B. P.; Leong, K. W. Scaffolding in Tissue Engineering: General Approaches and Tissue-Specific Considerations. *Eur. Spine J.* **2008**, *17*, 467.

(3) Rezwan, K.; Chen, Q. Z.; Blaker, J. J.; Boccaccini, A. R. Biodegradable and Bioactive Porous Polymer/Inorganic Composite Scaffolds for Bone Tissue Engineering. *Biomaterials* **2006**, *27*, 3413−3431.

(4) Armentano, I.; Dottori, M.; Fortunati, E.; Mattioli, S.; Kenny, J. M. Biodegradable Polymer Matrix Nanocomposites for Tissue Engineering: A Review. *Polym. Degrad. Stab.* **2010**, *95*, 2126−2146.

(5) Sergi, R.; Bellucci, D.; Cannillo, V. A review of bioactive glass/natural polymer composites: state of the art. *Materials* **2020**, *13*, 5560.

(6) Yuan, S.; Li, S.; Zhu, J.; Tang, Y. Additive Manufacturing of Polymeric Composites from Material Processing to Structural Design. *Composites, Part B* **2021**, *219*, No. 108903.

(7) Kaniuk, Ł.; Stachewicz, U. Development and Advantages of Biodegradable PHA Polymers Based on Electrospun PHBV Fibers for Tissue Engineering and Other Biomedical Applications. *ACS Biomater. Sci. Eng.* **2021**, DOI: 10.1021/acsbiomaterials.1c00757.

(8) Akbarzadeh, R.; Yousefi, A. M. Effects of Processing Parameters in Thermally Induced Phase Separation Technique on Porous Architecture of Scaffolds for Bone Tissue Engineering. *J. Biomed. Mater. Res., Part B* **2014**, *102*, 1304−1315.

(9) Wang, W.; Zhang, B.; Li, M.; Li, J.; Zhang, C.; Han, Y.; Wang, L.; Wang, K.; Zhou, C.; Liu, L.; Fan, Y.; Zhang, X. 3D Printing of PLA/n-HA Composite Scaffolds with Customized Mechanical Properties and Biological Functions for Bone Tissue Engineering. *Composites, Part B* **2021**, *224*, No. 109192.

(10) Gerhardt, L. C.; Boccaccini, A. R. Bioactive Glass and Glass-Ceramic Scaffolds for Bone Tissue Engineering. *Materials* **2010**, *3*, 3867−3910.

(11) Vallet-Regí, M.; González-Calbet, J. M. Calcium Phosphates as Substitution of Bone Tissues. *Prog. Solid State Chem.* **2004**, *32*, 1−31.

(12) Prati, C.; Gandolfi, M. G. Calcium Silicate Bioactive Cements: Biological Perspectives and Clinical Applications. *Dent. Mater.* **2015**, *31*, 351−370.

(13) Brunetti, L.; Degli Esposti, M.; Morselli, D.; Boccaccini, A. R.; Fabbri, P.; Liverani, L. Poly(Hydroxyalkanoate)s Meet Benign Solvents for Electrospinning. *Mater. Lett.* **2020**, *278*, No. 128389.

(14) Gandolfi, M. G.; Gardin, C.; Zamparini, F.; Ferroni, L.; Esposti, M. D.; Parchi, G.; Ercan, B.; Manzoli, L.; Fava, F.; Fabbri, P.; Prati, C.; Zavan, B. Mineral-Doped Poly(L-Lactide) Acid Scaffolds Enriched with Exosomes Improve Osteogenic Commitment of Human Adipose-Derived Mesenchymal Stem Cells. *Nanomaterials* **2020**, *10*, 432.

(15) Forni, M.; Bernardini, C.; Zamparini, F.; Zannoni, A.; Salaroli, R.; Ventrella, D.; Parchi, G.; Esposti, M. D.; Polimeni, A.; Fabbri, P.; Fava, F.; Prati, C.; Gandolfi, M. G. Vascular Wall−Mesenchymal Stem Cells Differentiation on 3d Biodegradable Highly Porous Casi-Dcpd Doped Poly (α-Hydroxy) Acids Scaffolds for Bone Regeneration. *Nanomaterials* **2020**, *10*, 243.

(16) Bellucci, D.; Sola, A.; Gentile, P.; Ciardelli, G.; Cannillo, V. Biomimetic Coating on Bioactive Glass-Derived Scaffolds Mimicking Bone Tissue. *J. Biomed. Mater. Res., Part A* **2012**, *100*, 3259−3266.

(17) Du, M.; Chen, J.; Liu, K.; Xing, H.; Song, C. Recent Advances in Biomedical Engineering of Nano-Hydroxyapatite Including Dentistry, Cancer Treatment and Bone Repair. *Composite, Part B Eng.* **2021**, *215*, No. 108790.

(18) Duan, Z.; Thomas, N. L. Water Vapour Permeability of Poly(Lactic Acid): Crystallinity and the Tortuous Path Model. *J. Appl. Phys.* **2014**, *115*, 064903.

(19) Degli Esposti, M.; Chiellini, F.; Bondioli, F.; Morselli, D.; Fabbri, P. Highly Porous PHB-Based Bioactive Scaffolds for Bone Tissue Engineering by in Situ Synthesis of Hydroxyapatite. *Mater. Sci. Eng. C* **2019**, *100*, 286−296.

(20) Bellucci, D.; Cannillo, V. A Novel Bioactive Glass Containing Strontium and Magnesium with Ultra-High Crystallization Temperature. *Mater. Lett.* **2018**, *213*, 67−70.

(21) Mehrali, M.; Moghaddam, E.; Shirazi, S. F. S.; Baradaran, S.; Mehrali, M.; Latibari, S. T.; Metselaar, H. S. C.; Kadri, N. A.; Zandi, K.; Osman, N. A. A. Synthesis, Mechanical Properties, and in Vitro Biocompatibility with Osteoblasts of Calcium Silicate-Reduced Graphene Oxide Composites. *ACS Appl. Mater. Interfaces* **2014**, *6*, 3947−3962.

(22) Schindelin, J.; Arganda-Carreras, I.; Frise, E.; Kaynig, V.; Longair, M.; Pietzsch, T.; Preibisch, S.; Rueden, C.; Saalfeld, S.; Schmid, B.; Tinevez, J. Y.; White, D. J.; Hartenstein, V.; Eliceiri, K.; Tomancak, P.; Cardona, A. Fiji: An Open-Source Platform for Biological-Image Analysis. *Nat. Methods* **2012**, *9*, 676−682.

(23) Ente Nazionale Italiano di Unificazione. *UNI EN 1936:2007, Natural Stone Test Methods - Determination of Real Density and Apparent Density, and of Total and Open Porosity*. 2007.
(24) Gassner, F.; Owen, A. J. Some Properties OfPoly(3-Hydroxybutyrate)-Poly(3-Hydroxyvalerate) Blends. *Polym. Int.* **1996**, *39*, 215−219.
(25) Crescenzi, V.; Manzini, G.; Calzolari, G.; Borri, C. Thermodynamics of Fusion of Poly-β-Propiolactone and Poly-ϵ-Caprolactone. Comparative Analysis of the Melting of Aliphatic Polylactone and Polyester Chains. *Eur. Polym. J.* **1972**, *8*, 449−463.
(26) International Organization for Standardization. ISO 10993-1:2009, *Biological Evaluation of Medical Devices - Part 1: Evaluation and Testing within a Risk Management Process*. 2009.
(27) International Organization for Standardization. ISO 10993-12:2012, *Biological Evaluation of Medical Devices - Part 12: Sample Preparation and Reference Materials*. 2012.
(28) International Organization for Standardization. ISO 10993-5:2009, *Biological Evaluation of Medical Devices - Part 5: Tests for in Vitro Cytotoxicity*. 2009.
(29) Misra, S. K.; Valappil, S. P.; Roy, I.; Boccaccini, A. R. Polyhydroxyalkanoate (PHA)/Inorganic Phase Composites for Tissue Engineering Applications. *Biomacromolecules* **2006**, *7*, 2249−2258.
(30) Maquet, V.; Boccaccini, A. R.; Pravata, L.; Notingher, I.; Jérôme, R. Porous Poly(α-Hydroxyacid)/Bioglass® Composite Scaffolds for Bone Tissue Engineering. I: Preparation and in Vitro Characterisation. *Biomaterials* **2004**, *25*, 4185−4194.
(31) Thein-Han, W. W.; Misra, R. D. K. Biomimetic Chitosan-Nanohydroxyapatite Composite Scaffolds for Bone Tissue Engineering. *Acta Biomater.* **2009**, *5*, 1182−1197.
(32) Zeinali, R.; Del Valle, L. J.; Torras, J.; Puiggalí, J. Recent Progress on Biodegradable Tissue Engineering Scaffolds Prepared by Thermally-Induced Phase Separation (Tips). *Int. J. Mol. Sci.* **2021**, *22*, 3504.
(33) Gandolfi, M. G.; Zamparini, F.; Degli Esposti, M.; Chiellini, F.; Aparicio, C.; Fava, F.; Fabbri, P.; Taddei, P.; Prati, C. Polylactic Acid-Based Porous Scaffolds Doped with Calcium Silicate and Dicalcium Phosphate Dihydrate Designed for Biomedical Application. *Mater. Sci. Eng. C* **2018**, *82*, 163−181.
(34) Gandolfi, M. G.; Zamparini, F.; Degli Esposti, M.; Chiellini, F.; Fava, F.; Fabbri, P.; Taddei, P.; Prati, C. Highly Porous Polycaprolactone Scaffolds Doped with Calcium Silicate and Dicalcium Phosphate Dihydrate Designed for Bone Regeneration. *Mater. Sci. Eng. C* **2019**, *102*, 341−361.
(35) Bassi, A.; Gough, J.; Zakikhani, M.; Downes, S. Bone Tissue Regeneration. In *Electrospinning for Tissue Regeneration*; Bosworth, L., Downes, S., Eds.; WOODHEAD Publishing, 2011; pp. 93−110.
(36) Vitale-Brovarone, C.; Verné, E.; Robiglio, L.; Appendino, P.; Bassi, F.; Martinasso, G.; Muzio, G.; Canuto, R. Development of Glass-Ceramic Scaffolds for Bone Tissue Engineering: Characterisation, Proliferation of Human Osteoblasts and Nodule Formation. *Acta Biomater.* **2007**, *3*, 199−208.
(37) Perez, R. A.; Mestres, G. Role of Pore Size and Morphology in Musculo-Skeletal Tissue Regeneration. *Mater. Sci. Eng. C* **2016**, *61*, 922−939.
(38) Karageorgiou, V.; Kaplan, D. Porosity of 3D Biomaterial Scaffolds and Osteogenesis. *Biomaterials* **2005**, *26*, 5474−5491.
(39) Martínez-Pérez, C. A.; Olivas-Armendariz, I.; Castro-Carmona, J. S.; García-Casillas, P. E. Scaffolds for Tissue Engineering Via Thermally Induced Phase Separation. In *Advances in Regenerative Medicine*; Wislet, S., Ed.; INTECH, 2011.
(40) Jack, K. S.; Velayudhan, S.; Luckman, P.; Trau, M.; Grøndahl, L.; Cooper-White, J. The Fabrication and Characterization of Biodegradable HA/PHBV Nanoparticle-Polymer Composite Scaffolds. *Acta Biomater.* **2009**, *5*, 2657−2667.
(41) Ma, P. X.; Zhang, R. Microtubular Architecture of Biodegradable Polymer Scaffolds. *J. Biomed. Mater. Res.* **2001**, *56*, 469−477.
(42) Zhang, R.; Ma, P. X. Poly(Alpha-Hydroxyl Acids)/Hydroxyapatite Porous Composites for Bone-Tissue Engineering. I. Preparation and Morphology. *J. Biomed. Mater. Res.* **1999**, *44*, 446−455.
(43) Wei, G.; Ma, P. X. Structure and Properties of Nano-Hydroxyapatite/Polymer Composite Scaffolds for Bone Tissue Engineering. *Biomaterials* **2004**, *25*, 4749−4757.
(44) Kothapalli, C. R.; Shaw, M. T.; Wei, M. Biodegradable HA-PLA 3-D Porous Scaffolds: Effect of Nano-Sized Filler Content on Scaffold Properties. *Acta Biomater.* **2005**, *1*, 653−662.
(45) Sultana, N.; Khan, T. H. In Vitro Degradation of PHBV Scaffolds and NHA/PHBV Composite Scaffolds Containing Hydroxyapatite Nanoparticles for Bone Tissue Engineering. *J. Nanomater.* **2012**, *2012*, 1.
(46) Salerno, A.; Di Maio, E.; Iannace, S.; Netti, P. A. Tailoring the Pore Structure of PCL Scaffolds for Tissue Engineering Prepared via Gas Foaming of Multi-Phase Blends. *J. Porous Mater.* **2012**, *19*, 181−188.
(47) Keller, T. S. Predicting the Compressive Mechanical Behavior of Bone. *J. Biomech.* **1994**, *27*, 1159−1168.
(48) Öhman, C.; Baleani, M.; Pani, C.; Taddei, F.; Alberghini, M.; Viceconti, M.; Manfrini, M. Compressive Behaviour of Child and Adult Cortical Bone. *Bone* **2011**, *49*, 769−776.
(49) Røhl, L.; Larsen, E.; Linde, F.; Odgaard, A.; Jørgensen, J. Tensile and Compressive Properties of Cancellous Bone. *J. Biomech.* **1991**, *24*, 1143−1149.
(50) Chodak, I. Polyhydroxyalkanoates: Origin, Properties and Applications. In *Monomers, Polymers and Composites from Renewable Resources*; Belgacem, M. N., Gandini, A., Eds.; Elsevier, 2008.
(51) Gorustovich, A. A.; Roether, J. A.; Boccaccini, A. R. Effect of Bioactive Glasses on Angiogenesis: A Review of In Vitro and In Vivo Evidences. *Tissue Eng., Part B* **2010**, *16*, 199−207.
(52) Mao, L.; Xia, L.; Chang, J.; Liu, J.; Jiang, L.; Wu, C.; Fang, B. The Synergistic Effects of Sr and Si Bioactive Ions on Osteogenesis, Osteoclastogenesis and Angiogenesis for Osteoporotic Bone Regeneration. *Acta Biomater.* **2017**, *61*, 217−232.
(53) Maeno, S.; Niki, Y.; Matsumoto, H.; Morioka, H.; Yatabe, T.; Funayama, A.; Toyama, Y.; Taguchi, T.; Tanaka, J. The Effect of Calcium Ion Concentration on Osteoblast Viability, Proliferation and Differentiation in Monolayer and 3D Culture. *Biomaterials* **2005**, *26*, 4847−4855.
(54) Penido, M. G. M. G.; Alon, U. S. Phosphate Homeostasis and Its Role in Bone Health. *Pediatr. Nephrol.* **2012**, *27*, 2039−2048.
(55) Hoppe, A.; Güldal, N. S.; Boccaccini, A. R. A Review of the Biological Response to Ionic Dissolution Products from Bioactive Glasses and Glass-Ceramics. *Biomaterials* **2011**, *32*, 2757−2774.
(56) O'Neill, E.; Awale, G.; Daneshmandi, L.; Umerah, O.; Lo, K. W. H. The Roles of Ions on Bone Regeneration. *Drug Discovery Today* **2018**, *23*, 879−890.
(57) Cacciotti, I. Bivalent Cationic Ions Doped Bioactive Glasses: The Influence of Magnesium, Zinc, Strontium and Copper on the Physical and Biological Properties. *J. Mater. Sci.* **2017**, *52*, 8812−8831.
(58) Bellucci, D.; Salvatori, R.; Giannatiempo, J.; Anesi, A.; Bortolini, S.; Cannillo, V. A New Bioactive Glass/Collagen Hybrid Composite for Applications in Dentistry. *Materials* **2019**, *12*, No. 2079.
(59) Bellucci, D.; Salvatori, R.; Anesi, A.; Chiarini, L.; Cannillo, V. SBF Assays, Direct and Indirect Cell Culture Tests to Evaluate the Biological Performance of Bioglasses and Bioglass-Based Composites: Three Paradigmatic Cases. *Mater. Sci. Eng. C* **2019**, *96*, 757−764.
(60) Sergi, R.; Bellucci, D.; Salvatori, R.; Maisetta, G.; Batoni, G.; Cannillo, V. Zinc Containing Bioactive Glasses with Ultra-High Crystallization Temperature, Good Biological Performance and Antibacterial Effects. *Mater. Sci. Eng. C* **2019**, *104*, No. 109910.
(61) Sergi, R.; Bellucci, D.; Salvatori, R.; Anesi, A.; Cannillo, V. Chitosan-Based Bioactive Glass Gauze. *Materials* **2020**, *13*, No. 2819.
(62) Bellucci, D.; Veronesi, E.; Dominici, M.; Cannillo, V. On the in Vitro Biocompatibility Testing of Bioactive Glasses. *Materials* **2020**, *13*, No. 1816.
(63) Sergi, R.; Cannillo, V.; Boccaccini, A. R.; Liverani, L. Incorporation of Bioactive Glasses Containing Mg, Sr, and Zn in

Electrospun PCL Fibers by Using Benign Solvents. *Appl. Sci.* **2020**, *10*, 5530.
(64) Bellucci, D.; Veronesi, E.; Strusi, V.; Petrachi, T.; Murgia, A.; Mastrolia, I.; Dominici, M.; Cannillo, V. Human Mesenchymal Stem Cell Combined with a New Strontium-Enriched Bioactive Glass: An Ex-Vivo Model for Bone Regeneration. *Materials* **2019**, *12*, No. 3633.
(65) Lin, K.; Xia, L.; Gan, J.; Zhang, Z.; Chen, H.; Jiang, X.; Chang, J. Tailoring the Nanostructured Surfaces of Hydroxyapatite Bioceramics to Promote Protein Adsorption, Osteoblast Growth, and Osteogenic Differentiation. *ACS Appl. Mater. Interfaces* **2013**, *5*, 8008−8017.
(66) Zhao, L.; Liu, L.; Wu, Z.; Zhang, Y.; Chu, P. K. Effects of Micropitted/Nanotubular Titania Topographies on Bone Mesenchymal Stem Cell Osteogenic Differentiation. *Biomaterials* **2012**, *33*, 2629−2641.
(67) Zhu, L.; Luo, D.; Liu, Y. Effect of the Nano/Microscale Structure of Biomaterial Scaffolds on Bone Regeneration. *Int. J. Oral Sci.* **2020**, *12*, 1−15.
(68) Cui, H.; Sinko, P. J. The Role of Crystallinity on Differential Attachment/Proliferation of Osteoblasts and Fibroblasts on Poly (Caprolactone-Co-Glycolide) Polymeric Surfaces. *Front. Mater. Sci.* **2012**, *6*, 47−59.
(69) Washburn, N. R.; Yamada, K. M.; Simon, C. G.; Kennedy, S. B.; Amis, E. J. High-Throughput Investigation of Osteoblast Response to Polymer Crystallinity: Influence of Nanometer-Scale Roughness on Proliferation. *Biomaterials* **2004**, *25*, 1215−1224.
(70) Groussard, C.; Morel, I.; Chevanne, M.; Monnier, M.; Cillard, J.; Delamarche, A. Free Radical Scavenging and Antioxidant Effects of Lactate Ion: An in Vitro Study. *J. Appl. Physiol.* **2000**, *89*, 169−175.

https://doi.org/10.1021/acsapm.2c00270
ACS Appl. Polym. Mater. 2022, 4, 4306−4318